PHYSICAL REVIEW B **68**, 180101(R) (2003)

Long-term correlations distinguish coarsening mechanisms in alloys

Lorenz-M. Stadler,[1,*] Bogdan Sepiol,[1] Richard Weinkamer,[2] Markus Hartmann,[2] Peter Fratzl,[2] Jan W. Kantelhardt,[3] Federico Zontone,[4] Gerhard Grübel,[4] and Gero Vogl[1]

[1]*Institut für Materialphysik, Universität Wien, Strudlhofgasse 4, A-1090 Wien, Austria*

[2]*Max-Planck-Institute of Colloids and Interfaces, Department of Biomaterials, D-14424 Potsdam, Germany*

[3]*Institut für Theoretische Physik III, Justus-Liebig-Universität Giessen, Heinrich-Buff-Ring 16, D-35392 Giessen, Germany*

[4]*European Synchrotron Radiation Facility, BP 220, F-38043 Grenoble Cedex, France*

(Received 11 July 2003; published 3 November 2003)

We determine long-term correlations in the time series of fluctuating x-ray speckle intensities. A fluctuation analysis of small angle x-ray scattering data of the two phase-separating alloys Al-6 at. %Ag and Al-9 at. %Zn at late stages of phase separation reveals long-term correlations that are dramatically different for the two systems. From a comparison with recent Monte Carlo simulations we conclude that two different coarsening mechanisms are predominant in the two alloys—coarsening either by diffusion of single atoms or by movement of whole precipitates.

DOI: 10.1103/PhysRevB.68.180101 PACS number(s): 61.10.−i, 64.75.+g, 81.40.−z

There is a long-standing debate about how precipitate coarsening in phase-separating alloys can proceed. Recent Monte Carlo (MC) simulations[1,2] showed different predominant coarsening mechanisms depending on the preferred location of vacancies. If vacancies are preferably found in the matrix, coarsening will proceed via diffusion of individual atoms from smaller precipitates to larger ones. This is the classical Lifshitz-Slyozov-Wagner (LSW) mechanism. In the case of a coagulation mechanism,[3] whole precipitates move and coalesce. The mobility of whole precipitates will be enhanced, if vacancies are preferably localized in the precipitates or on their surfaces. To discriminate between different coarsening mechanisms experimentally is difficult, but has become feasible with the availability of coherent x rays and the method of x-ray photon correlation spectroscopy (XPCS), where in contrast to electron microscopy investigations information about processes in a large sample volume is gained. Therefore, in the aforementioned MC study by Weinkamer and Fratzl,[2] time dependent speckle intensities corresponding to an XPCS experiment in a small angle x-ray scattering (SAXS) geometry were simulated for each coarsening mechanism. A fluctuation analysis of the fluctuating speckle intensities resulted in characteristically different long-term correlations for the two coarsening mechanisms.

XPCS relies on the fact that scattering of coherent radiation from a disordered sample produces a highly modulated diffraction pattern, commonly referred to as a speckle pattern.[4] This interference pattern is in direct relation to the positions of scattering centers in the coherently illuminated material. If their positions change, the corresponding speckle pattern will also be modified, and the speckle intensity will fluctuate in time. By analyzing the temporal correlations of this intensity fluctuation, XPCS yields information about the dynamics in the material. By using coherent x rays instead of visible light an almost atomic resolution can be achieved.[5]

A frequently used approach to evaluate XPCS data is to calculate correlation functions of the time-dependent intensity of a single speckle. For investigating equilibrium dynamics the calculation of the autocorrelation function is sufficient, since then only the time interval between measurements is relevant.[6–8] For nonequilibrium systems a two-time correlation function has to be applied[9,10] because the dynamics additionally depends on the absolute time. The correlation-function technique works well if short-term correlations are investigated, e.g., exponentially decaying correlations, and correlation times that are characteristic for the underlying dynamics can be gained. The situation changes, however, if long-term correlations are present, i.e., correlations with an autocorrelation function $C(t)$ proportional to $t^{-\gamma}$, with $0<\gamma<1$ and t the time leading to a diverging correlation time. Especially on longer time scales it becomes very difficult to resolve the correlation behavior unambiguously by calculating $C(t)$ directly. The latter attempt is even more delicate in the presence of statistical noise. These problems can be overcome by applying the fluctuation analysis (FA) technique, which was introduced as ''DNA walk'' when spatial long-range correlations in nucleotide sequences were detected.[11] Here we report on the successful detection of long-term correlations in an XPCS experiment by applying FA, allowing one to distinguish between different coarsening mechanisms in two phase-separating binary alloys at late stages of phase separation.

We performed XPCS experiments at the undulator beamline ID10A at the ESRF, Grenoble[12] in SAXS (transmission) geometry with two phase-separating systems, Al-6 at. %Ag at 140 °C and Al-9 at. %Zn at 0 °C. Both are well known model systems for precipitate growth,[13,14] where the minority component forms precipitates. Due to small lattice misfits, spherical precipitates with the same lattice structure as the matrix are found. Evaluating the reduced temperature T/T_c, where the critical temperature for the miscibility gap, T_c, is taken from the equilibrium phase diagram, yields ≈ 0.55 for the Al-6 at. %Ag and ≈ 0.61 for the Al-9 at. %Zn measurement. This means that the measurements are both well comparable between each other and performed at reduced temperatures where no coarsening mechanism is excluded by theory.[15]

To ensure that our samples were in the coarsening regime of phase separation, samples were first homogenized for 48 h at 550 °C (Al-6 at. %Ag) and for 135 min at 400 °C (Al-9

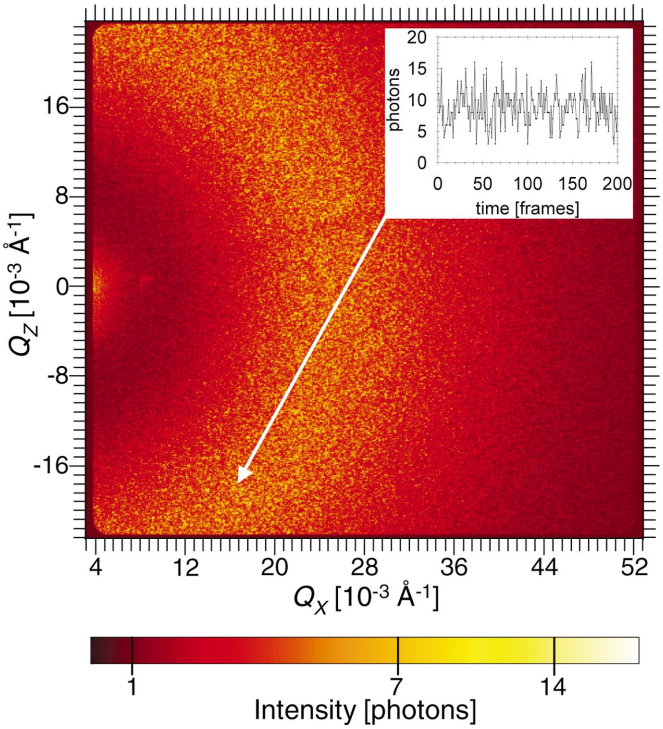

FIG. 1. (Color) SAXS spectrum of Al-6 at. %Ag, logarithmic intensity scale. The inset shows the fluctuating intensity in one single pixel, indicated by the arrow.

at. %Zn), respectively. Afterwards Al-6 at. %Ag was annealed at the measurement temperature of 140 °C for 47 h, Al-9 at. %Zn at 0 °C for 82 h. In contrast to recent measurements of Livet *et al.*[10] and Malik *et al.*,[9] respectively, our experiments were performed in quasi-equilibrium, i.e., the sample temperature was low enough to prevent significant precipitate growth during a single measurement, which lasted a few hours. In all cases SAXS spectra taken before and after the XPCS measurements did not show any change, i.e., the mean precipitate size did not change measurably. Assuming spherical shape the mean precipitate radius r could be derived from the SAXS data, yielding for Al-6 at. %Ag, $r=7$ nm, and for Al-9 at. %Zn, $r=3$ nm.

The x-ray energy, selected by a Si(111) monochromator, was 8 keV, corresponding to a wavelength of 1.55 Å. An energy resolution of $\Delta E/E=10^{-4}$ and a circular pinhole aperture of diameter $d=12$ μm approximately 20 cm upstream of the sample were used to provide a temporally and spatially coherent x-ray beam. Estimated values were 1.55 μm for the longitudinal length, 4 μm for the horizontally transversal length and about 150 μm for the vertically transversal coherence length.[12] A guard slit in front of the sample was used to eliminate parasitic scattering from the pinhole. Sample thicknesses were 46 μm for Al-6 at. %Ag and 70 μm for Al-9 at. %Zn, respectively.

Time series of up to $N=8192$ speckle patterns (''frames'') were taken with a direct illumination CCD camera (Princeton Instruments, 1242×1152 pixels, pixel size 22.5 ×22.5 μm^2) mounted on a table in 2.3 m distance from the sample.[9] Figure 1 shows a SAXS diffraction pattern of Al-6 at. %Ag. The ring-like structure is caused by isotropic shape and arrangement of precipitates. Because of the very small beam diameter (12 μm) and large grain sizes (50–100 μm diameter) of the polycristalline samples, practically only single crystalline domains were probed by the x-ray beam. The inset of Fig. 1 demonstrates the intensity fluctuations in one pixel, corresponding to a single speckle, during 200 consecutive frames. When measuring near the SAXS maximum the exposure time was typically 1 sec. To save readout time and to cover the largest possible range of the scattering vector Q, rectangular regions of interest with $\Delta Q_x \gg \Delta Q_z$ were chosen, thus allowing a total repetition rate of one frame per 1.65 s. Since the whole CCD detector covered a maximum Q range of 0.049 Å^{-1}, up to three consecutive measurements with different, slightly overlapping positions of the CCD camera were performed. The maximum Q range was limited to about 0.18 Å^{-1} due to insufficient scattering intensity for larger Q.

The time evolution of the intensity in each specific pixel was analyzed by FA. For this we calculate

$$F^2(t)=\langle (Y_{j+t}-Y_j)^2\rangle \quad \text{with} \quad Y_j=\sum_{k=1}^{j}\Delta I_k . \qquad (1)$$

Here, $\Delta I_k=I_k-\langle I\rangle$, where I_k is the intensity in a pixel in the kth time bin and $\langle I\rangle=1/N\Sigma_{k=1}^{N}I_k$ is the mean intensity. The angular brackets in Eq. (1) represent the average over all pairs with the same time lag t. Repeating this procedure for all t between 1 and $N-1$, the squared fluctuation function $F^2(t)$ is obtained. Statistics is improved by averaging the FA results over all pixels with the same Q. In general $F^2(t)$ can be well fitted by a power law $F^2(t)\propto t^{2\alpha}$. The fluctuation exponent α is related to the correlation exponent γ by $\alpha=1-\gamma/2$ with $0<\gamma<1$.[16] This means that long-term correlations are present if $\alpha>0.5$.[18]

One can understand the FA evaluation procedure in complete analogy to the random walk of a particle in one dimension in space. Calculating Y_j would give the particle position if ΔI_k denoted the step of the particle at time step k. $F^2(t)$ would be the corresponding mean-square displacement after t time steps. Assuming random uncorrelated motion, after t time steps the mean-square displacement $F^2(t)$ would be given by the well-known Einstein relation $F^2(t)=2Dt^{2\alpha}$ with $\alpha=0.5$ and D the diffusivity. But if diffusion becomes anomalous, i.e., the random walk is accelerated on all time scales, the movement becomes long-term correlated and the mean-square displacement grows faster than linear with time, yielding $\alpha>0.5$.

Figure 2 shows typical results of the fluctuation analysis of the Al-6 at. %Ag data for a small, a medium, and a large Q value, normalized to Q_{max} where the maximum scattering intensity was found. As can be seen a power law over several decades is observed for $F(t)$. To obtain the fluctuation exponent α for each Q, we fitted only the data for $t<N/10$, which is a save upper limit.[16] For the two upper curves in Fig. 2, fits yield a fluctuation exponent $\alpha>0.5$, indicating *long-term correlations* in the data. Only on short time scales does $F(t)$ deviate from the fit. There, in both cases the fluctuation exponent seems to be ≈ 0.5, which corresponds to random uncorrelated fluctuations. The domination of noise at

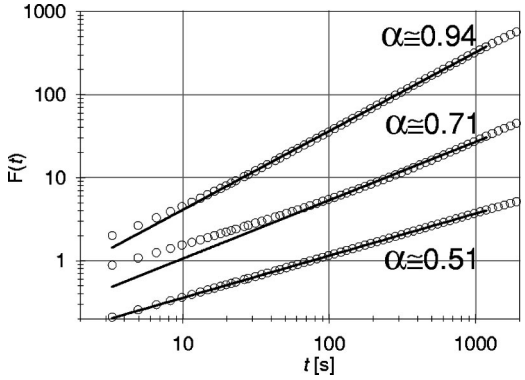

FIG. 2. Al-6 at. %Ag: double-logarithmic plot of three typical $F(t)$ curves at different Q, that were fitted $\propto t^{\alpha}$ (straight lines). Top curve at $Q/Q_{max}=0.73$, middle curve at $Q/Q_{max}=2.39$, and bottom curve at $Q/Q_{max}=3.72$.

small t is due to the limited intensity in our experiment. The inset in Fig. 1 shows that even in the SAXS maximum the intensity is rather low, yielding a relatively high fraction of uncorrelated background noise. Due to the summation in the FA procedure these uncorrelated fluctuations cancel on longer time scales, where the intrinsic long-term correlated fluctuations dominate the scaling behavior, yielding $\alpha > 0.5$. Therefore, long-term correlations are detected only on larger time scales.

Figure 3 shows the collected fluctuation exponents α versus Q/Q_{max}. Data from both samples show long-term correlations—with a different dependence on the scattering vector Q. It is evident that α is varying with Q more slowly around the maximum for Al-6 at. %Ag than for Al-9 at. %Zn—the plateau (indicated by the dotted line) is more pronounced in case of Al-6 at. %Ag. Also curvatures at values of Q/Q_{max} between 1.5 and 3 are remarkably different. This behavior is reminiscent of previous MC simulations,

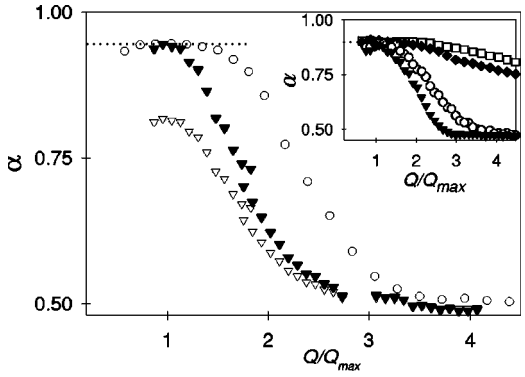

FIG. 3. Fluctuation exponent α vs Q/Q_{max}. Error bars from fits are smaller than symbols. Al-6 at. %Ag, circles. Al-9 at. %Zn, triangles; full triangles scaled to the maximum value for Al-6 at. %Ag are shown for comparison. Dotted line indicates maximum plateau. Inset: fluctuation exponents from MC simulations (Ref. 2): Coarsening via LSW mechanism, squares; with scaled intensity plus background, circles. Coarsening via coagulation mechanism, full diamonds; with scaled intensity plus background, full triangles. Note the good agreement between circles and full triangles, respectively, in the figure and the inset.

where a connection between the Q dependence of α and the predominant coarsening mechanism was established.[2] Comparison with these first simulation results yields already a rough, qualitative agreement, see the inset of Fig. 3, squares and full diamonds. It appears that in Al-6 at. %Ag at 140 °C the LSW mechanism dominates the coarsening. In case of Al-9 at. %Zn at 0 °C results indicate coarsening via the coagulation mechanism.

The main difference between $\alpha(Q)$ curves for the two coarsening mechanisms can be explained in the following simple-minded picture. At medium values of Q/Q_{max}, structures in real space are probed on a length scale which compares to the average precipitate size. Precipitate movement, in case of coarsening via coagulation, implies rather strong shape changes of single precipitates due to the rearrangement of atoms on precipitate surfaces—causing weaker correlations than in the LSW case, where the shape of single precipitates remains practically unchanged when single atoms evaporate from the precipitate surface. At low Q vectors, structures in real space are probed on even larger length scales. There, no details of precipitate shape—particularly no shape changes—are visible, which yields highly correlated signals.

In order to emulate experimental conditions in the MC calculations, simulated intensities were scaled to the measured intensity maximum of Al-6 at. %Ag for coarsening via the LSW mechanism and to the intensity maximum of Al-9 at. %Zn for coagulation. Additionally one photon was added with a probability of 50% to simulated intensities at each time step, corresponding quantitatively to the measured uncorrelated background. The fluctuation exponents from FA of these intensities form an unambiguous fingerprint for the two coarsening mechanisms, see inset Fig. 3, circles (LSW mechanism) and full triangles (coagulation mechanism). Exactly this fingerprint is also found in the curves for Al-6 at. %Ag, circles, and Al-9 at. %Zn, full triangles, where the data of Al-9 at. %Zn is scaled to the maximum of Al-6 at. %Ag for better comparability. The qualitative agreement between experiment and simulation is excellent. Our conclusion is that different coarsening mechanisms account for the different dependence of the fluctuation exponent α on the scattering vector: for Al-6 at. %Ag at 140 °C a dominating LSW mechanism, and for Al-9 at. %Zn at 0 °C coarsening preferably via the coagulation mechanism.

To find an explanation for different coarsening mechanisms, it is instructive to estimate vacancy positions roughly by considering the melting temperatures of the alloy constituents.[1] If the melting temperature of the precipitating constituent is lower than that of the matrix, vacancies will rather be found in the precipitates than in the matrix, and vice versa. Considering the melting temperature T_m of each alloy constituent—$T_m^{Al}=933$ K, $T_m^{Ag}=1234$ K and $T_m^{Zn}=693$ K—gives a hint for a more prominent role of the coagulation mechanism in Al-9 at. %Zn than in Al-6 at. %Ag.[1]

Figure 3 obviously also shows quantitative differences between XPCS and MC results, which can be explained as follows: In the experiment, the absolute values of α cannot exactly be determined by applying FA because trends in the overall intensity, which are caused, for example, by the de-

cay of the electron beam in the synchrotron storage ring, can adulterate them.[16] This may be the reason why the $\alpha(Q)$ curve of Al-6 at. %Ag lies above the original one of Al-9 at. %Zn. In addition, coherence conditions in the experiment can never be as perfect as in simulations. In any case, the variation of α with Q is unaffected by such trends or less coherence, making the qualitative distinction between the two coarsening mechanisms possible.

On the other hand a constraint in MC simulations is the limited system size which limits also the size of the precipitate diameter to about 5 nm. Since it is crucial for our considerations that the system is already in the coarsening regime, in the experiment precipitation diameters are larger, 14 nm for Al-6 at. %Ag and 6 nm for Al-9 at. %Zn, respectively. Theoretical considerations predict a decreasing importance of the coagulation mechanism with increasing precipitate size,[3,17] which also makes a coagulation mechanism in Al-9 at. %Zn more probable than in Al-6 at. %Ag. The considerations above make clear that an exact quantitative match between the results for α from simulations and the experiment cannot be expected. In fact, a perfect numerical match is not necessary to discriminate between the different coarsening mechanisms because a reasonable qualitative distinction is possible due to an unambiguous fingerprint in the corresponding $\alpha(Q)$ curves.

In conclusion, we successfully applied fluctuation analysis to data of an x-ray photon correlation spectroscopy experiment. Actually, we do find long-term correlations in our data, as predicted by Monte Carlo simulations[2] for coarsening in binary phase-separating systems at late stages of phase separation. A qualitative agreement between experimental and simulation results enables us to draw conclusions about the underlying coarsening mechanism in a direct way, which is promising for future investigations.

The authors are indebted to O. Paris for helpful discussions concerning SAXS measurements, to B. Pfau for assistance during the experiment, and to C. Motz and G. Zickler for sample characterization. This work was financially supported by the project GZ 45.529/4-VI/6a/2002 of the Austrian Federal Ministry for Education, Science and Culture.

*Email address: lstadler@ap.univie.ac.at

[1] J.-M. Roussel and P. Bellon, Phys. Rev. B **63**, 184114 (2001).
[2] R. Weinkamer and P. Fratzl, Europhys. Lett. **61**, 261 (2003).
[3] K. Binder and D. Stauffer, Phys. Rev. Lett. **33**, 1006 (1974).
[4] M. Sutton, E.E. Nagler, S.G. Mochrie, T. Greytak, L.E. Bermann, G. Held, and G.B. Stephenson, Nature (London) **352**, 608 (1991).
[5] G. Grübel and G. Vogl, Synchrotron Radiat. News **15**, 14 (2002).
[6] D.O. Riese, W.L. Vos, G.H. Wegdam, F.J. Poelwijk, D.L. Abernathy, and G. Grübel, Phys. Rev. E **61**, 1676 (2000).
[7] T. Thurn-Albrecht, W. Steffen, A. Patkowski, G. Meier, E.W. Fischer, G. Grübel, and D.L. Abernathy, Phys. Rev. Lett. **77**, 5437 (1996).
[8] S.G.J. Mochrie, A.M. Mayes, A.R. Sandy, M. Sutton, S. Brauer, G.B. Stephenson, D.L. Abernathy, and G. Grübel, Phys. Rev. Lett. **78**, 1275 (1997).
[9] A. Malik, A.R. Sandy, L.B. Lurio, G.B. Stephenson, S.G.J. Mochrie, I. McNulty, and M. Sutton, Phys. Rev. Lett. **81**, 5832 (1998).
[10] F. Livet, F. Bley, R. Caudron, E. Geissler, D. Abernathy, C. Detlefs, G. Grübel, and M. Sutton, Phys. Rev. E **63**, 036108 (2001).
[11] C.-K. Peng, S.V. Buldyrev, A.L. Goldberger, S. Havlin, F. Sciortino, M. Simons, and H.E. Stanley, Nature (London) **356**, 168 (1992).
[12] D.L. Abernathy, G. Grübel, S. Brauer, I. McNulty, G.B. Stephenson, S.G.J. Mochrie, A.R. Sandy, N. Mulders, and M. Sutton, J. Synchrotron Radiat. **5**, 37 (1998).
[13] F. Langmayr, P. Fratzl, and G. Vogl, Acta Metall. Mater. **40**, 3381 (1992).
[14] K. Osamura, H. Okuda, Y. Amemiya, and H. Hashizume, Metall. Mater. Trans. A **19A**, 1973 (1988).
[15] T.T. Rautiainen and A.P. Sutton, Phys. Rev. B **59**, 13 681 (1999).
[16] J.W. Kantelhardt, E. Koscielny-Bunde, H.H.A. Rego, S. Havlin, and A. Bunde, Physica A **295**, 441 (2001).
[17] P. Fratzl and O. Penrose, Phys. Rev. B **55**, R6101 (1997).
[18] Note that the nonstandard definition $F^2(t) \propto t^{\alpha}$ was used in Ref. 2, leading to exponents α there larger by a factor of 2.